

FY2014 Partner User Activity Report

Application of Synchrotron Radiation in Materials Crystallography

Bo Iversen<sup>1</sup>, Jacob Overgaard<sup>1</sup>, Yoshihiro Kuroiwa<sup>2</sup>, Eiji Nishibori<sup>3</sup>

<sup>1</sup>Department of Chemistry, University of Aarhus, Aarhus, Denmark

<sup>2</sup>Graduate School of Science, Hiroshima University, Japan

<sup>3</sup>Faculty of Pure and Applied Sciences, University of Tsukuba, Japan

(1)

Initial PU Proposal No. / Beamline Name	2014A0078 / BL02B1										
PU Project Leader (Affiliation)	Bo Iversen (University of Aarhus)										
Research Experiment	Application of Synchrotron Radiation in Materials Crystallography										
Collaboration for Beamline Facility Upgrade	Structural dynamics infrastructure development and its leading use										
User Support	Help and support to the users using upgraded beamline facilities										
Research Term	14A	14B	15A	15B	16A	16B	17A	17B	18A	18B	Total
Number of Shifts Used	44.5	56.875	45	38.75	42	38.875	41.75	47.625	43.75	48	447.125
Number of Supported Proposals	3	1	5	1	1	2	1	2	1	1	18

(2) Overview of partner user activities

1) Initial goal for the PU program

The original priority for the Aarhus group in the Partner User Proposal was to establish that the beamline BL02B1 could consistently deliver high quality, high resolution, and low-temperature diffraction data of the utmost quality, for the purpose of charge density (CD) refinement using the multipole model. During this work, we used the molecular system, Rubrene, as benchmark system and we have continued to use this system extensively also following the end of this PU proposal. In addition, we performed accurate studies of inorganic compounds, such as transition metal sulfides, alkali salts, and intermetallic compounds in the realm of thermoelectric and 2D materials. Extraordinary results were obtained for van der Waals material TiS<sub>2</sub>. It was also a priority to develop methods for light induced excited state crystallography. This relied on the access to a fast detector, which was investigated together with a research group in Nancy, France, and later with a commercial HPAD-detector from Dectris. We examined the use of a photon counting pixelated detector on the beamline BL02B1.

Time-resolved diffraction (TR-XRD) was addressed by PU member Prof. Yoshihiro Kuroiwa from Hiroshima University, as it was proposed by SPring-8 that it should be possible to make TR-XRD experiments under applied electric field at the BL02B1.

Finally, the initial proposal included plans by the Nishibori group to endow BL02B1 with capabilities for non-ambient crystallography. One of these was the development of high-pressure (HP) infrastructure at the beamline.

2) Collaboration for beamline upgrades

For CD studies, X-ray diffraction data require good statistics. The large cylindrical IP camera has successfully been used to collect high quality data having a large dynamic range and large area using a 1 shot image method. However, the disadvantage of the IP detector is its long readout- and erase-time, which is more than 8 minutes per image. We initially tried to evaluate a photon counting pixelated detector, imXPAD, to replace the IP for CD study. This was done together with University de Lorraine, including all the hardware and software adaptations that are required. Eventually, we could collect image data of

standard samples with imXPAD for CD study. Our plan was to measure a set of very accurate Bragg intensities on BL02B1 on an  $\text{YTiO}_3$  perovskite type crystal using 35 keV radiation, and analyze the performance of the XPAD detector knowing that the detector chip is made from silicon.

Eventually, it was concluded that the high energy at the BL02B1 is not compatible with the Si-based detector chip in the imXPAD. At the time when this was carried out, the development of CdTe or AsGa intermetallic semiconductor materials was still in its infancy and not commercially available for large detectors, but this has since been altered, culminating in the purchase of a new CdTe detector by SPring-8 for installation at BL02B1.

In January 2018, a new PILATUS3 X CdTe detector was installed at BL02B1 by beamline scientist Dr. Kunihisa Sugimoto, and we used beamtime in 2018A and 2018B to very thoroughly investigate the capabilities of this detector. Initially, we attempted to adapt the new detector frame format to the existing Rigaku RAPID-AUTO software, but this was quickly abandoned, and instead we developed frame conversion software to enable the use of Bruker Apex3 software for data reduction. The detector control and subsequent software is now readily available for all users at the beamline. These results are now in press in *Journal of Applied Crystallography*<sup>[26]</sup>.

Prior to the introduction of the pixel-detector at BL02B1, the PU team developed the TR-XRD system, in which the timing of X-ray irradiation was synchronized with the RF signal of

SPring-8. Figure 1 shows the schematic image of the TR-XRD system used for a ferroelectric material  $\text{BaTiO}_3$ . We have succeeded in capturing the change in crystal structure of  $\text{BaTiO}_3$  during the polarization reversal by the pump-probe method using the chopped SR pulse X-rays of 30 keV from the train bunch in the D-mode operation with the temporal resolution of 685 ns. In the initial stage, the cyclic periods of applying AC and irradiating pulse X-rays are both the same 1 kHz. This system enabled us to collect a data set to reveal the intrinsic structural change in  $\text{BaTiO}_3$  in 3 hrs. The incident X-ray intensity lost by the windows of X-ray chopper was negligible since the X-rays were well focused at the X-ray chopper at BL02B1. Using the tandem chopper system we tried to eliminate X-rays with higher energy more efficiently. However, half of the incident X-rays was lost at the windows of the choppers. In the current chopper system which we have developed, it is best to experiment with a single chopper using X-rays up to 30 keV. The chopped SR pulse X-rays from the single bunch in the H-mode operation with the temporal resolution of 50 ps was successfully obtained using the TR-XRD system for the focused X-rays, and was used for the quartz crystal. A data set for the crystal structure analysis was collected in 6 hrs. In this experiment, we have achieved to upgrade the TR-XRD system better to support any AC frequency.

$\alpha$ -quartz is a high-Q material. The resonant frequency is very sensitive to the sample thickness and the condition of the electronic anodes. In this sample, a clear resonant vibration was observed for

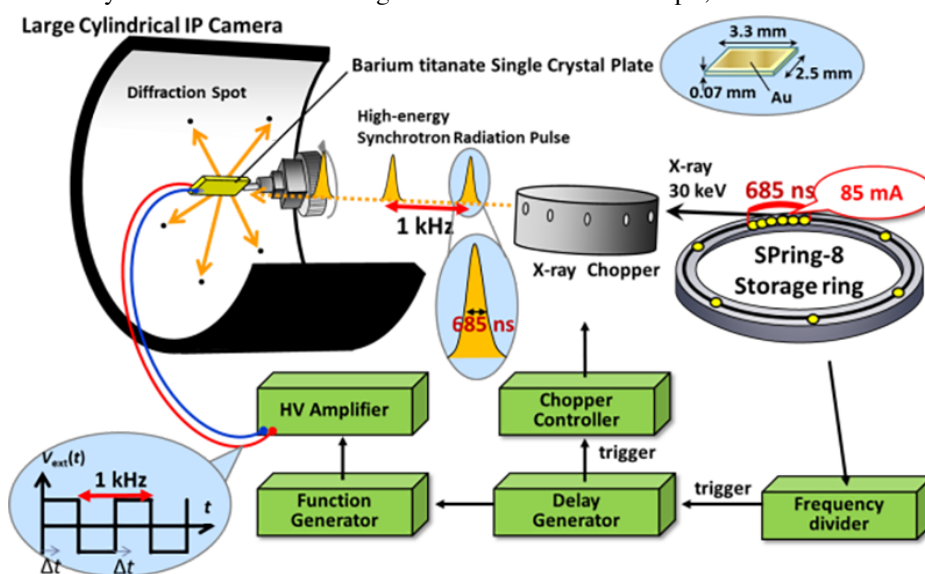


Figure 1 Time-resolved X-ray diffraction (TR-XRD) system for the D-mode operation. The system is available for any bunch modes using the focused X-rays.

the 30.05 MHz AC frequency. No significant resonant vibration could be observed for the 30.00 and 30.10 MHz AC. In fact, it is very difficult to prepare the quartz sample with a certain resonant frequency. The resonant frequency changes with small changes in the thickness of sample and electrode, and reproducible sample fabrication is difficult. Therefore, we upgrade the TR-XRD system to better support any AC frequency higher than 1 MHz. This improvement was achieved by a clever combination of the X-ray chopper and the programmed function generator, and applied to the quartz experiments. Nowadays, this technique is adopted in the time-resolved XMCD measurements for the magnetic materials excited by pulsed RF field at BL39XU (N. Kikuchi *et al.*: *IEEE Transactions on Magnetics*, DOI: 10.1109/TMAG.2017.2745211), and more in BL25SU.

For the non-ambient crystallographic investigations, Dr. Sugimoto installed a diamond anvil cell (DAC) and a pressure measurement system during the 2014A period. Prof. Nishibori advised convenient tools, such as a syringe for pressure medium, and a glue to fix gasket, for the DAC experiment. In addition, experimental procedures for single crystal DAC experiments were fully developed. Of particular importance was the problem of centering of sample for which a method was conceived. The reason that centering is problematic even though the crystal is visible through the diamond anvils is that the refractive index of diamond is high, so it is very difficult center the DAC using the already installed CCD camera system. Instead, we developed a centering method using an X-Y stage attached to a goniometer head. Finally, Dr. Sugimoto developed an automatic sampling system using a z-stage of CCD camera in collaboration with the partners.

### 3) Research Results related to Upgraded Beamline

#### 3-a) Charge Density Results on Rubrene

One of our first results from BL02B1 was the CD of the organic semiconductor material, rubrene. This was published in *IUCrJ*<sup>[3]</sup>, in which we addressed the link between bulk properties and the microscopic CD. This relied on being able to determine small deviations in CD, which was possible due to the high data quality. The comparison of thermal parameters from X-rays and neutron experiments showed the best agreement ever found for an X-N study. The study also included

use of novel interaction descriptors such as the non-covalent indicator (Figure 2). This study represents the fulfilment of the first priority in the beamline upgrade. As part of the work, we established a strategy for data collection that was able to cover the full reciprocal space in the minimum amount of time, and optimizing the time with crystal exposure relative to image plate readout. These procedures were later adopted by other users.

#### 3-b) Charge Density results on a Single Molecule Magnet.

We have successfully reduced the absorption in the samples by increasing the X-ray energy. Now, we are frequently using 50 keV radiation, and this seems to defer the crystal decay to the extent that some experiments are now possible. This is particularly successful for coordination complexes where the effect of decay seems to be most prevalent. We have thus managed to collect high-resolution CD data on the single molecule magnet  $\text{Dy}(\text{dbm})_3(\text{bpy})$ , where dbm = dibenzoylmethane, and for the first time managed to obtain an experimental model for the 4f valence density distribution in  $\text{Dy}^{3+}$ . In a first approximation, the electronic structure of a  $\text{Dy}^{3+}$  can be described as a pure  $m_J = \pm 15/2$  state, which has a strongly oblate valence density distribution and very axial magnetic properties, while mixing of higher lying states into the

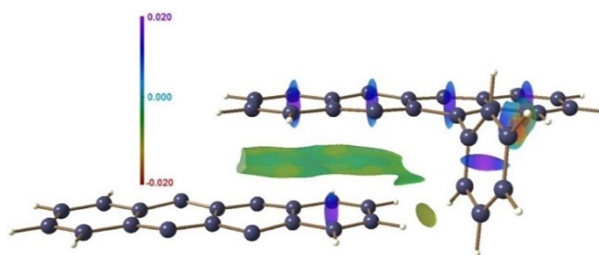


Figure 2 The NCI surface separating the dimers in the  $\text{Cr} \dots \text{Cr}$  stacking interaction in rubrene.

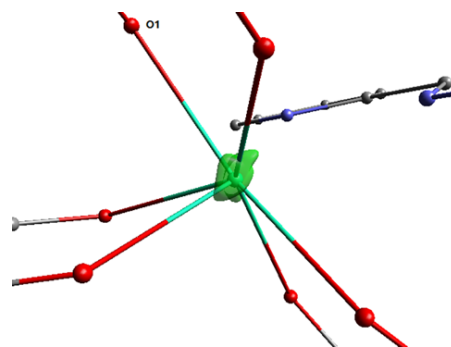


Figure 3 Isosurface of the density from the multipoles of the 4f CD around Dy in  $\text{Dy}(\text{dbm})_3(\text{bpy})$ .

ground state will perturb this lucid picture. We find clear deviations from the oblate density using the CD model using a multipole model including  $l = 6$  terms to describe the  $f$ -electrons, as shown in Figure 3. The results indicate clearly that the approximation of a pure ground state is not reproduced in the experimental CD. The level of theory used in our study are expensive high-level state-of-the-art multiconfigurational calculations, which are also used throughout the molecular magnetic community, but our results indicate that they may not be accurate enough to reproduce the true, mixed electronic structure.

### 3-c) Charge Density in N-H-N Hydrogen Bond

$\text{H}_3\text{Co}(\text{CN})_6$  exhibits one of the shortest N-H-N hydrogen bonds in the literature, which shows strong isotope dependence. To investigate and quantify this isotope and temperature dependence, we studied the CD on both the hydrogenated and the deuterated compounds at different temperatures. The CD study will contribute with important knowledge about hydrogen bonds, which is a very important research topic with implications within fields such as enzyme catalysis and molecular self-assembly.

The structure presents a challenge for CD studies due to symmetry and light elements, and very accurate X-ray diffraction data are required. Thus, high-resolution X-ray diffraction data has been collected on both hydrogenated and deuterated samples at both 20 K and 100 K, up to  $1.7 \text{ \AA}^{-1}$  for the 20 K data and to  $1.4 \text{ \AA}^{-1}$  for the 100 K data and with high redundancy in all cases. To determine the hydrogen positions and thermal parameters accurately, the X-ray data were combined with high quality neutron powder diffraction data. The X-ray data has been modelled using the multipole model and analyzed using topological analysis. This indicates a double-covalently bonded hydrogen, which has never previously been observed in an N-H-N hydrogen bond (Figure 4). The behavior

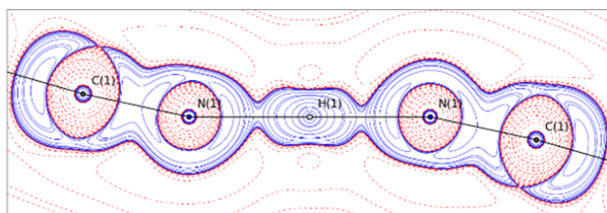


Figure 4 Laplacian of total electron density in the N-H-N plane of  $\text{H}_3\text{Co}(\text{CN})_6$ .

is very similar to what is observed in the O-H-O Low Barrier Hydrogen Bond (LBHB) in benzoylacetone, but in the present case the hydrogen bond seems to be even more symmetric. The cobalt atom shows a clear redistribution of charge as usually observed in an octahedrally coordinated transition metal complex, but with some degree of covalency in the Co-C bond. Many density-based observables are very similar to what is observed in a series of transition metal carbonyls, which is interesting as one would expect much more ionic character of the Co-CN bond from the formal charges of the atoms.

### 3-d) Installing and implementing a HPAD detector at BL02B1

The latest development was the implementation of the PILATUS3 X 1M CdTe detector at BL02B1. After successfully converting data to a usable format, it was found that both very strong and very weak data suffered from systematic errors. The problem was identified as being due to the fact that the given official specifications of the detector count rate is related to the instantaneous flux, not the total count across a whole peak. This results in systematic differences in strong intensities for different incoming beam flux, and the internal count-rate correction was found to be inadequate. Only significant beam attenuation for the collection of strong reflections has proven to circumvent this systematic error. Similarly, the estimated uncertainties of the very weak intensities are hampered by the use of particular programs, and we have also developed a routine to avoid these problems. These results have just been submitted. At the same time, we are continuing to work closely together with the detector manufacturer, Dectris, to investigate their latest Eiger detector, in which some of the unnoticed intrinsic errors have been eradicated. A detailed account of this work is currently in press.

### 4) User Support relating to Upgrade

In the PU support program, the PU group applied the upgraded TR-XRD system to quartz, in which the chopped SR pulse X-rays of 35 keV from the single bunch in the H-mode operation with the temporal resolution of 50 ps and the cyclic period of 26.1 kHz were used. The transient atomic displacements during a resonant thickness-shear vibration of the quartz are revealed under applied AC electric field.

The TR-XRD experiments carried out using the hybrid AC field is schematically shown in Figure 5 (Top). The AC field with 30.05 MHz was applied to the sample 1,000 times for 33  $\mu$ s. After the 5  $\mu$ s break, the AC field was applied again and repeated. The pulse X-rays are irradiated at the appropriated timing in the 995th cycle of the 1,000 cycle where the stable resonance were observed.

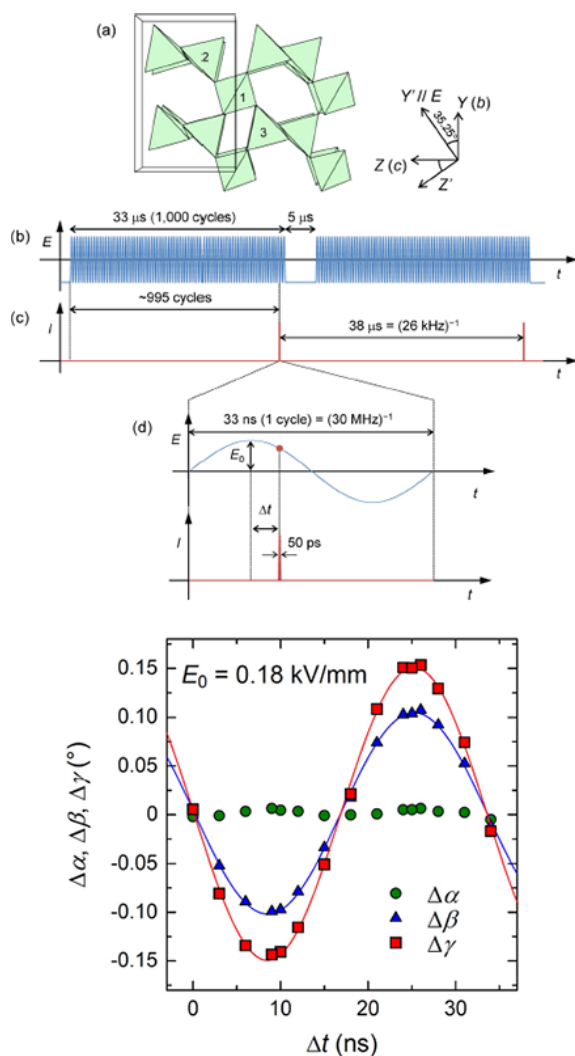


Figure 5 (Top) Crystal structure of  $\alpha$ -quartz and schematic of the hybrid alternating electric field and repetitive short-pulse X-rays for TR-XRD. (a) Crystal structure of right  $\alpha$ -quartz viewed along the X-axis. (b) An applied electric field consisting of 1,000 cycles of a 30 MHz sine wave and repetitions at 26.1 kHz. (c) Short-pulse X-rays with a pulse width of 50 ps and a repetitive frequency of 26.1 kHz. (d) Relationship between a cycle of the sine-wave electric field and an X-ray pulse. (Bottom) Time changes of the  $\alpha$ ,  $\beta$ , and  $\gamma$  angles in quartz under the resonant AC field.

Time changes of the  $\alpha$ ,  $\beta$ , and  $\gamma$  angles under the resonant AC field are indicated in Figure 5 (Bottom). The lattice strain resonantly amplified by the AC electric field is  $\sim 104$  times larger than that induced by a static electric field. The resonantly amplified lattice strain is achieved by fast displacements of oxygen anions and collateral resilient deformation of Si–O–Si angles bridging rigid SiO<sub>4</sub> tetrahedra, which efficiently transduce electric energy into elastic energy.

### 5) Concluding remarks

We have developed experimental procedures that allow collection of the most accurate single crystal X-ray diffraction data ever making beamline BL02B1 the premier facility for accurate crystallographic studies in the world. The exceptional quality of the data obtained from an IP detector was demonstrated in crystals containing weak chemical interactions such as  $\pi$ - $\pi$ -bonding, hydrogen bonding or van der Waals-bonding. We now need to spread the possibilities more generally in the crystallographic community and the results have opened up possibilities for high impact chemical bonding studies. We have introduced the imXPAD detector based on a Si-based detector chip and collected many data sets. However, the data quality was not sufficient for CD studies and CdTe based detectors are required. It was, however, essential to establish that the new CdTe detector can measure data of similar accuracy as the IP detector. In the case of metal organic crystals severe crystal decay was previously observed and this presents a general problem prohibiting studies using the image-plate setup. The solution was found with the faster detector technology, such as the PILATUS photon counting detector from the Dectris company being installed primo 2018.

We have developed the TR-XRD system with X-ray choppers synchronized with the RF signal of SPring-8. We upgraded the TR-XRD system better to support AC frequencies higher than 1 MHz. However, the current X-ray chopper is mainly designed for the D-mode operation. We will start to install the new X-ray chopper designed for the H-mode operation from 2018A. The design is already completed and much higher efficiency in collecting data with 50 ps temporal resolution is expected. The self-evaluation of goal achievement in the TR-XRD part should be 80%, because the new X-ray

chopper designed suitable for the H-mode operation is not installed at the moment.

We have obtained accurate HP CD results of diamond using DAC as shown in Figure 6. The R-values of multipole refinement are around 2% with  $d > 0.35 \text{ \AA}$  data. However, it is still difficult to detect pressure dependence of strength of chemical bonding. We need higher quality data for the quantitative CD study including pressure dependence.

Finally, a workshop was held for all PU members in Tsukuba (see Figure 7 for a snapshot from the meeting). The participants included the Aarhus University group (Bo Iversen, Jacob Overgaard), the Grabowsky group from University of Bremen, Germany as well as scientists from SPring-8 BL02B1 and the single crystal beam line of J-PARC. We had a lively discussion of various topics that had appeared of importance over the lifetime of the PU project, such as benefits of a new detector, synergy of multiple facility use and so on. The meeting was very valuable and it contributes to the continuous development of the beamline.

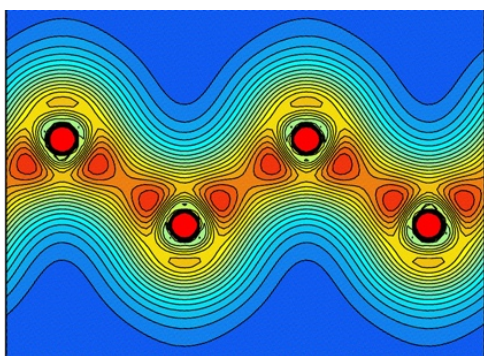


Figure 6 Valence CD of Diamond under 1.1 GPa pressure using DAC.



Figure 7 Discussion at PU-organized workshop in Tsukuba.

### (3) List of papers (refereed papers)

- [ 1 ] SPring-8 publication ID = 28292  
M. Shimada *et al.* "Optical Properties of Disilane-Bridged Donor-Acceptor Architectures: Strong Effect of Substituents on Fluorescence and Nonlinear Optical Properties" *Journal of the American Chemical Society* **137** (2015) 1024-1027.
- [ 2 ] SPring-8 publication ID = 29616  
R. Iizuka *et al.* "Large Electric-field-induced Strain in Pseudo-cubic  $\text{BaTiO}_3\text{-Bi}(\text{Mg}_{0.5}\text{Ti}_{0.5})\text{O}_3\text{-BiFeO}_3$  Ceramics" *Transactions of the Materials Research Society of Japan* **40** (2015) 295-299.
- [ 3 ] SPring-8 publication ID = 29703  
V. Hathwar *et al.* "Quantitative Analysis of Intermolecular Interactions in Orthorhombic Rubrene" *IUCrJ* **2** (2015) 563-574.
- [ 4 ] SPring-8 publication ID = 31142  
Y. Ishii *et al.* "Two Competing Soft Modes and an Unusual Phase Transition in the Stuffed Tridymite-type Oxide  $\text{BaAl}_2\text{O}_4$ " *Physical Review B* **93** (2016) 134108.
- [ 5 ] SPring-8 publication ID = 31416  
E. Magome *et al.* "Role of Structure Gradient Region on Dielectric Properties in  $\text{Ba}(\text{Zr},\text{Ti})\text{O}_3\text{-KNbO}_3$  Nanocomposite Ceramics" *Japanese Journal of Applied Physics* **54** (2015) 10NB04.
- [ 6 ] SPring-8 publication ID = 31419  
H. Tanaka *et al.* "Metal-Semiconductor Transition Concomitant with a Structural Transformation in Tetrahedrite  $\text{Cu}_{12}\text{Sb}_4\text{S}_{13}$ " *Journal of the Physical Society of Japan* **85** (2016) 014703.
- [ 7 ] SPring-8 publication ID = 33183  
M. Sist *et al.* "Carrier Concentration Dependence of Structural Disorder in Thermoelectric  $\text{Sn}_{1-x}\text{Te}$ " *IUCrJ* **3** (2016) 377-388.
- [ 8 ] SPring-8 publication ID = 34006  
M. Sist *et al.* "Low-Temperature Anharmonicity in Cesium Chloride ( $\text{CsCl}$ )" *Angewandte Chemie International Edition* **56** (2017) 3625-3629.
- [ 9 ] SPring-8 publication ID = 34819  
S. Ogura *et al.* "Antiferromagnetic Ordering in the Single-Component Molecular Conductor  $[\text{Pd}(\text{tmdt})_2]$ " *Inorganic Chemistry* **55** (2016) 7709-7716.
- [10] SPring-8 publication ID = 34830  
K. Qian *et al.* "Does the Thermal Evolution of Molecular Structures Critically Affect the Magnetic Anisotropy?" *Chemical Science* **6** (2015) 4587-4593.

- [11] SPring-8 publication ID = 35490  
M. Tsuchiya *et al.* “ $\beta$ -IminoBODIPY Oligomers: Facilely Accessible  $\pi$ -Conjugated Luminescent BODIPY Array” *Chemical Communications* **53** (2017) 7509-7512.
- [12] SPring-8 publication ID = 35492  
Y. Ogino *et al.* “Solvent-Controlled Doublet Emission of an Organometallic Gold(I) Complex with a Polychlorinated Diphenyl(4-pyridyl)methyl Radical Ligand” *Inorganic Chemistry* **56** (2017) 3909-3915.
- [13] SPring-8 publication ID = 35556  
S. Nakajima *et al.* “A Fluorescent Microporous Crystalline Dendrimer Discriminates Vapour Molecules” *Chemical Communications* **54** (2018) 2534-2537.
- [14] SPring-8 publication ID = 35588  
M. Sist *et al.* “Low-Temperature Anharmonicity in Cesium Chloride (CsCl)” *Angewandte Chemie* **129** (2017) 3679-3683.
- [15] SPring-8 publication ID = 37143  
H. Kasai *et al.* “X-ray Electron Density Investigation of Chemical Bonding in van der Waals Materials” *Nature Materials* **17** (2018) 249-252.
- [16] SPring-8 publication ID = 37680  
T. Fujita *et al.* “Hydrothermal Reactor for in-situ Synchrotron Radiation Powder Diffraction at SPring-8 BL02B2 for Quantitative Design for Nanoparticle” *The Journal of Supercritical Fluids* **147** (2019) 172-178.
- [17] SPring-8 publication ID = 37681  
B. Zhou *et al.* “Single-Component Molecular Conductor [Pt(dmdt)<sub>2</sub>]-a Three-Dimensional Ambient-Pressure Molecular Dirac Electron System” *Chemical Communications* **55** (2019) 3327-3330.
- [18] SPring-8 publication ID = 38679  
T. Nakamura *et al.* “Bpytrisalen/Bpytrisaloph: A Triangular Platform That Spatially Arranges Different Multiple Labile Coordination Sites” *Inorganic Chemistry* **58** (2019) 7863-7872.
- [19] SPring-8 publication ID = 38680  
V. Hathwar *et al.* “Low-Temperature Structural Phase Transitions in Thermoelectric Tetrahedrite, Cu<sub>12</sub>Sb<sub>4</sub>S<sub>13</sub>, and Tennantite, Cu<sub>12</sub>As<sub>4</sub>S<sub>13</sub>” *Crystal Growth & Design* **19** (2019) 3979-3988.
- [20] SPring-8 publication ID = 39854  
C. Gao *et al.* “Observation of the Asphericity of 4f-electron Density and its Relation to the Magnetic Anisotropy Axis in Single-Molecule Magnets” *Nature Chemistry* **12** (2020) 213-219.
- [21] SPring-8 publication ID = 39855  
M. K. Thomsen *et al.* “Insights into Single-Molecule-Magnet Behavior from the Experimental Electron Density of Linear Two-Coordinate Iron Complexes” *Inorganic Chemistry* **58** (2019) 3211-3218.
- [22] SPring-8 publication ID = 39856  
P. C. Bunting *et al.* “A Linear Cobalt(II) Complex with Maximal Orbital Angular Momentum from a Non-Aufbau Ground State” *Science* **362** (2018) eaat7319.
- [23] SPring-8 publication ID = 39857  
J. Overgaard *et al.* “Magnetism and Variable Temperature and Pressure Crystal Structures of a Linear Oligonuclear Cobalt Bis-Semiquinonate” *Dalton Transactions* **45** (2016) 12924-12932.
- [24] SPring-8 publication ID = 39890  
M. W. Shi *et al.* “Measurement of Electric Fields Experienced by Urea Guest Molecules in the 18-Crown-6/Urea (1:5) Host-Guest Complex: An Experimental Reference Point for Electric-Field-Assisted Catalysis” *Journal of the American Chemical Society* **141** (2019) 3965-3976.
- [25] SPring-8 publication ID = 39891  
K. Tolborg *et al.* “Low barrier hydrogen bonds in negative thermal expansion material H<sub>3</sub>Co(CN)<sub>6</sub>” *Chemistry a European Journal* **25** (2019) 6814-6822.
- [26] SPring-8 publication ID = 39895  
L. Krause *et al.* “Accurate high-resolution single-crystal diffraction data from a Pilatus3 X CdTe detector” *Journal of Applied Crystallography* (2020) in press.